C. R. Palevol 12 (2013) 519–530

Contents lists available at ScienceDirect

Comptes Rendus Palevol

www.sciencedirect.com

General palaeontology, systematics and evolution (Vertebrate palaeontology)

# On the olfactory apparatus in the Miocene odontocete *Squalodon* sp. (Squalodontidae)

## *À propos de l'appareil olfactif de l'Odotoncète miocène* Squalodon *sp. (Squalodontidae)*

Stephen J. Godfrey[a,b,*]

[a] *Department of Paleontology, Calvert Marine Museum, PO Box 97, Solomons, MD 20688, USA*
[b] *National Museum of Natural History, Smithsonian Institution, Washington, DC, USA*

ARTICLE INFO

*Article history:*
Received 28 January 2013
Accepted after revision 28 March 2013
Available online 3 July 2013

Presented by Yves Coppens

*Keywords:*
Squalodontidae
Odontoceti
Olfaction
Miocene
Calvert Formation
Ethmoturbinates

*Mots clés :*
Squalodontidés
Odontocètes
Olfaction
Miocène
Formation Calvert
Ethmoturbinés

ABSTRACT

Most extant odontocetes appear to be anosmatic. However, some Miocene odontocetes, including a broken skull attributed to *Squalodon* sp. (Calvert Formation, Calvert Cliffs, Maryland, USA) preserve the osteological components associated with a well-developed sense of smell: dorsal nasal meatuses, ethmoturbinates within olfactory recesses, a perforate cribriform plate, and an olfactory bulb chamber. In *Squalodon* sp., the area within the olfactory recesses (i.e., covered in life by olfactory sensory epithelia) is 5367 $mm^2$ and the area occupied by the olfactory bulbs (i.e., the ethmoid area) is 769.8 $mm^2$. In most mammals, the area of the olfactory epithelium is typically circa 16 times larger than the ethmoid area. The area covered by olfactory epithelium in CMM-V-2287 is only about seven times larger than its ethmoid area, less than half the area in typical mammals. During the Miocene, most odontocetes variously lost the osteological proxies indicative of osmatic ability. Perhaps biosonar surpassed the efficiency of olfactory cues during predation and social/parental/sexual interactions rendering the latter redundant/obsolete in odontocete analysis of, and interactions with and within their aquatic environments.



RÉSUMÉ

La plupart des Odontocètes vivants semblent être anosmatiques. Cependant, certains Odotoncètes miocènes, incluant un crâne brisé attribué à *Squalodon* sp. (formation Calvert, Calvert Cliffs, Maryland, États-Unis), conservent des traits olfactifs associés à un sens de l'odorat bien développé : méats nasaux dorsaux, ethmoturbinaux dans les cavités olfactives, plaque perforée criblée et chambre bulbaire. Chez le *Squamodon* sp., la surface à l'intérieur des cavités olfactives (c'est-à-dire recouvertes, chez les animaux en vie, par les épithéliums sensoriels olfactifs) est de 5367 $mm^2$ et la surface occupée par les bulbes olfactifs (i.e. la surface de l'ethmoïde) est de 769,8 $mm^2$. Chez la plupart des mammifères, la surface de l'épithélium olfactif est environ 16 fois plus grande que celle de l'ethmoïde. La surface recouverte par l'épithélium olfactif dans l'échantillon CMM-V-2287 n'est que sept fois plus grande que celle de l'ethmoïde, moins de la moitié de cette surface chez les Mammifères typiques. Pendant le Miocène, la plupart des Odotoncètes perdent de manière variable les éléments

* Department of Paleontology, Calvert Marine Museum, PO Box 97, Solomons, MD 20688, USA.
*E-mail addresses:* Godfresj@co.cal.md.us, Godfrey.SJ@gmail.com

1631-0683/$ – see front matter 
http://dx.doi.org/10.1016/j.crpv.2013.03.002

indicatifs d'une capacité osmatique. Peut-être le biosonar a-t-il surpassé l'efficacité des signaux olfactifs pendant la prédation et les interactions sociales, parentales et sexuelles, rendant ces derniers redondants.



## 1. Introduction

Recent odontocetes have strongly telescoped crania with subvertical narial passages devoid of ethmoturbinate/olfactory recesses. In extant adult toothed whales that have been studied, the tissues that conduct olfaction are absent: there is no cranial nerve I, no olfactory bulbs, and no olfactory tracts (Breathnach, 1960; Edinger, 1955; Hoch, 2000; Oelschläger, 1992; Oelschläger and Oelschläger, 2009; Thewissen et al., 2011). Furthermore, less than 25% of the olfactory receptor genes remain intact, the majority having mutated into nonfunctional pseudogenes (Kishida et al., 2007; McGowen et al., 2008; Thewissen et al., 2011). Unlike extant odontocetes, baleen whales evidence an ability to smell, albeit greatly reduced as compared to land-dwelling mammals but better than that of humans (Cave, 1988; Edinger, 1955; Hoch, 2000; McGowen et al., 2008; Oelschläger and Oelschläger, 2009; Thewissen et al., 2011). These conclusions are based on the fact that baleen whales possess the bony features and soft tissues associated with osmatic ability as well as many genes that code for the detection of airborne odors (Godfrey et al., 2013; Kishida and Thewissen, 2012; Thewissen et al., 2011).

Although extant odontocetes seemingly have no ability to detect airborne odors, during the Oligocene and Miocene, many toothed whales still possessed the osteological proxies indicative of olfactory ability (Hoch, 2000). Among the fossil toothed whales found within the Miocene, Chesapeake Group, representatives of the Squalodontidae (Fig. 1), Squalodelphinidae, Platanistidae, and Eurhinodelphinidae preserve these features (crescentic foramina, ethmoturbinates within olfactory recesses, cribriform plate, and olfactory bulb chambers). A fragmented skull of *Squalodon* sp. (CMM-V-2287, Figs. 2–4) preserves an olfactory anatomy suggesting impressive olfactory sensitivity as compared to most other Neogene odontocetes. The purpose of this contribution is to more fully describe and attempt to rank its olfactory ability as compared to other cetaceans and mammals based solely on the size of the osteological proxies for olfactory ability. Although headway is made on both fronts, it would not yet seem possible to use these results to quantify its ability to: (1) detect a wide array of odorants (acuity); (2) detect them at low concentrations (sensitivity); and (3) distinguish similar odorants (discrimination).

**Institutional abbreviations**: CMM-V: Calvert Marine Museum vertebrate collection, Calvert County, Maryland; MGUH VP: Geological Museum of Copenhagen University; USNM: United States National Museum of Natural History, Smithsonian Institution, Washington, DC.

Anatomical terminology follows Sisson and Grossman (1953), Pihlström et al. (2005), Mead and Fordyce (2009), and Van Valkenburgh et al. (2011).

## 2. Systematic paleontology

CETACEA Brisson, 1762
PELAGICETI Uhen, 2008
NEOCETI Fordyce and de Muizon, 2003
ODONTOCETI Flower, 1867
Family Squalodontidae† Brandt, 1873

Squalodontidae is an entirely extinct family of odontocetes that display features typically associated with more archaic cetaceans, i.e., heterodonty (the possession of a diversity of tooth forms that include recognizable incisors, canines, and double-rooted cheek teeth) (Fordyce, 2009), and the osteological correlates associated with the ability to detect airborne odors. Within the Miocene Chesapeake Group, squalodontids are only known from the Calvert Formation (Dooley, 2003, 2005; Gottfried et al., 1994). Two species are currently recognized: *Squalodon calvertensis* Kellogg, 1923 (Fig. 1B) and *Squalodon whitmorei* Dooley, 2005 (Fig. 1A). CMM-V-2287 (Fig. 1C) most closely resembles *S. whitmorei*, primarily in its more robust proportions, although with a condylobasal length of only about 900 mm (see below), it is intermediate in size between the two. Based on morphological features, there is no doubt that CMM-V-2287 represents a third squalodontid from the Calvert Formation, but sorting out its identity vis-à-vis European squalodontids (Rothausen, 1968) is beyond the scope of this effort. However, that issue does not change the conclusions of this paper.

**Locality**: The skull of CMM-V-2287 (Figs. 2–4) broke into many pieces when much of it fell naturally from high in the cliffs at the Willows, Calvert County, Maryland, USA. What remained of the skull in the cliffs was subsequently quarried in situ.

**Formation and age**: CMM-V-2287 derives from Bed 10 of the Calvert Formation along Calvert Cliffs. Bed 10 is part of the Plum Point Member that spans the Burdigalian–Langhian boundary of the Middle Miocene. Therefore, the skull is approximately 16 million years old.

**Description**: In an anterior view of the ethmoid region of CMM-V-2287 (Fig. 2), two curved laterally concave apertures (i.e., the crescentic foramina; anteroposteriorly compressed and diminutive homologues of the mammalian dorsal nasal meatus) descend vertically into the olfactory recesses. The curving troughs are approximately 62 mm long (high), about 5.7 mm wide at their minimum and about 30 mm deep (anteroposterior depth). The crescentic foramina (dorsal nasal meatuses) communicate through their length with the subvertical internal nares. The crescentic foramina and the olfactory recesses constitute a diverticulum of the internal nares, lying entirely posterior to the unobstructed airway. Unlike the typical mammalian nose (Van Valkenburgh et al., 2011), there are no maxilloturbinates (i.e. turbinates originating from the

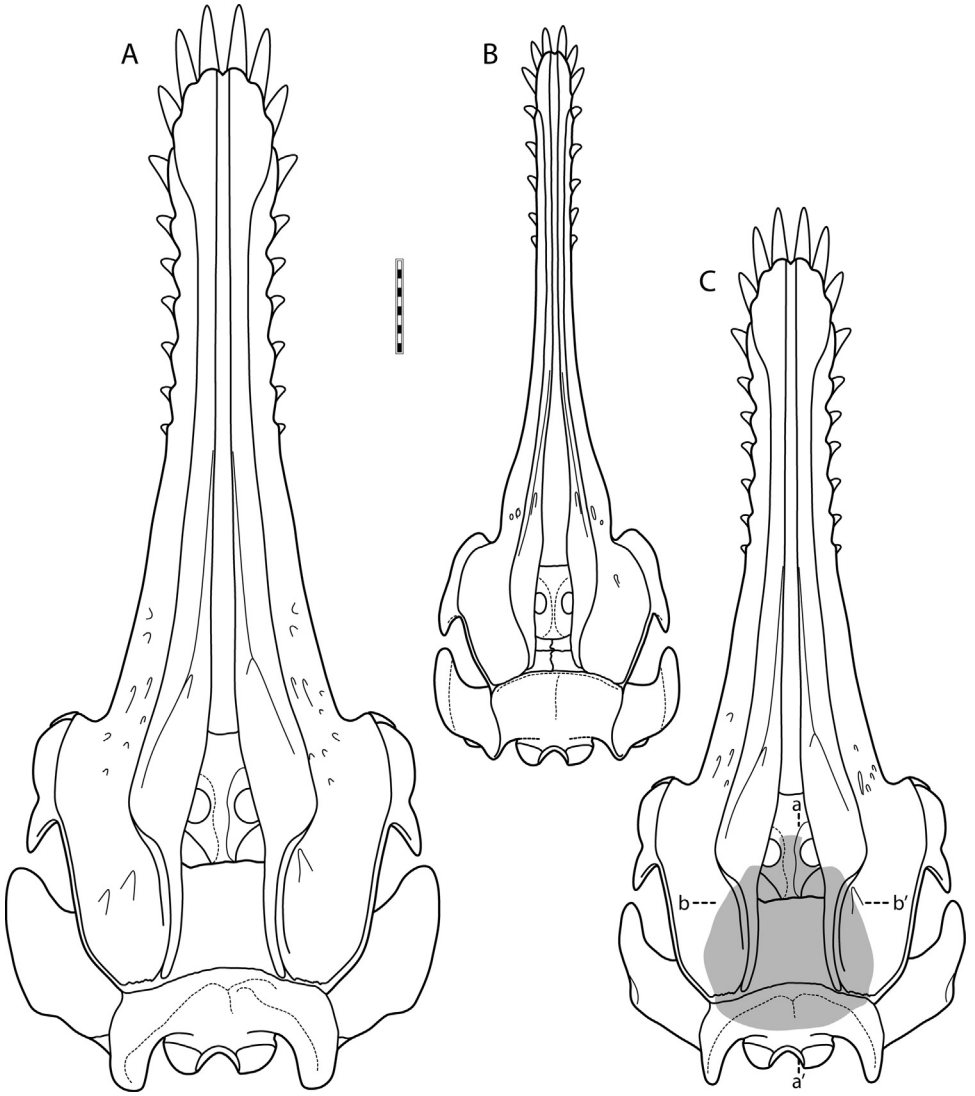


**Fig. 1.** Miocene squalodontids from the Calvert Formation, Maryland and Virginia, USA. A. Restoration of the skull of *Squalodon whitmorei* Dooley, in dorsal view. B. *Squalodon calvertensis* Kellogg. C. A preliminary restoration of *Squalodon* sp. CMM-V-2287, based mainly on *S. whitmorei*. Although much of the skull is preserved in CMM-V-2287, only the shaded region outlined here was the focus of this study. A line joining the two letters a and a' mark the parasagittal plane shown in Fig. 3A. Likewise, a line joining b and b' indicates the approximate position of the subvertical CT scan image shown in Fig. 3B. Scale bar equals 10 cm

**Fig. 1.** Squalodontidés miocènes de la formation Calvert, Maryland et Virginie, États-Unis. A. Restauration du crâne de *Squalodon whitmorei* Dooley en vue dorsale. B. *Squalodon calvertensis* Kellogg. C. Restauration préliminaire de *Squalodon* sp., CNN-V-2287, principalement basée sur *S. whitmorei*. Bien que la plus grande partie du crâne soit conservée dans CMM-V-2287, seule la zone ombrée est l'objet de notre étude. Une ligne joignant les lettres a et a' marque le plan parasagittal que montre la Fig. 3A. De la même façon, une ligne joignant b et b' indique la position approximative de l'image scan CT subverticale que montre la Fig. 3B. Barre d'échelle = 10 cm.

maxilla) or nasoturbinates (i.e., turbinates attached to the nasals) present in CMM-V-2287.

Within each essentially bilaterally symmetrical olfactory recess, 3–4 ethmoturbinates project into the lumen of this space (Figs. 2 and 3B). Unlike the scroll-shaped turbinates within the ethmoidal labyrinth in terrestrial mammals, the thick ethmoturbinates in CMM-V-2287 do not coil about their long axis. Their long axis nearly parallels that of the skull. One ethmoturbinate originates on the ventral floor of the recess, another one or two from its lateral wall and the third/fourth comprises the dorsomedial margin of the olfactory recess. These turbinates project dorsally, medially, and ventrally respectively into the olfactory recess.

The posteroventral floor of each olfactory recess (i.e., the ethmoid bone or cribriform plate) is perforated by numerous foramina of varying diameter (Figs. 2D, 3 and 4). These foramina conducted the primary olfactory axons that originated within the olfactory bulb chamber on the cerebral side of the cribriform plate. The olfactory bulb chamber (i.e., the ethmoid area) is subcylindrical, the long axis of which forms an angle of approximately 60° to the long

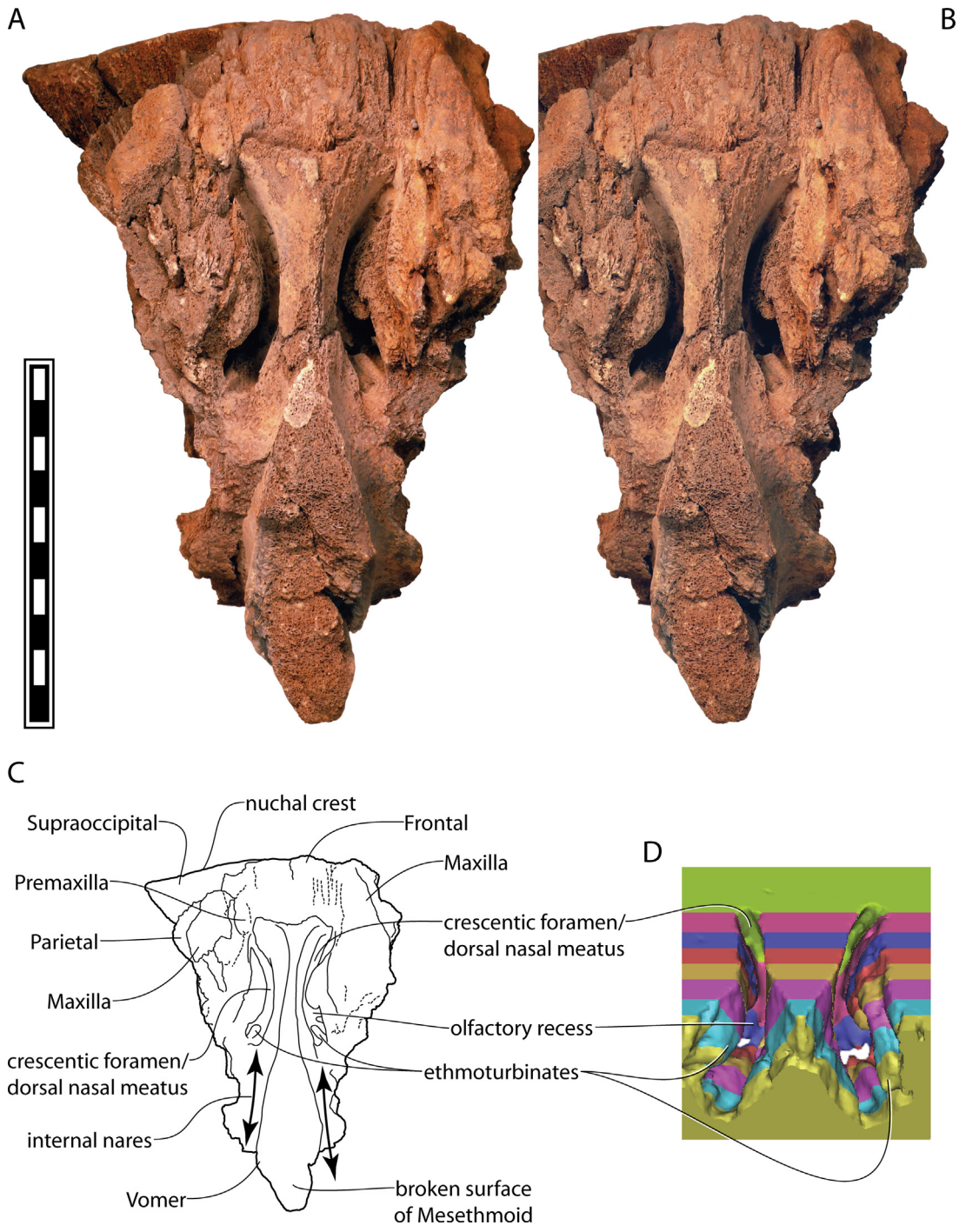


**Fig. 2.** A and B. Stereo pairs of a broken skull of *Squalodon* sp., CMM-V-2287, in an anterior view of the cranial vertex and surrounding bones. Below the vertex are the two bold crescentic foramina (dorsal nasal meatuses) at the base of which are the ethmoturbinate-bearing olfactory recesses. C. Interpretive line drawing showing the salient features of CMM-V-2287. D. An anterodorsal view of the olfactory recesses in CMM-V-2287 generated from CT scans in Mimics®. The olfactory recesses were isolated from the rest of the skull. The seven anterior colored layers are each 5 mm thick. The sections were generated in order to calculate the surface area of the olfactory epithelium covering the nasal ethmoturbinates. The white openings on the bottom of the olfactory recesses are perforations through the cribriform plate. Scale bar for A and B equals 10 cm.

**Fig. 2.** A et B. Couple stéréoscopique d'un crâne brisé de *Squalodon* sp., CMM-V-2287, en vue antérieure du vertex crânien et des os à l'entour. Au-dessous du vertex, bien apparents, les deux foramens en forme de croissants (méats nasaux dorsaux) à la base desquels se trouvent les cavités olfactives portant les ethmoturbinaux. C. Dessin au trait interprétatif montrant les traits marquants de CMM-V-2287. D. Vue antérodorsale des cavités olfactives dans CMM-V-2287, obtenue en scan CT en Mimicsr®. Les cavités olfactives ont été isolées du reste du crâne. Les sept feuillets antérieurs colorés ont chacun 5 mm d'épaisseur. Les coupes ont été effectuées pour calculer la surface de l'épithélium olfactif recouvrant les ethmoturbinaux nasaux. Les ouvertures blanches à la base des cavités olfactives sont des perforations au travers de la plaque criblée. Barre d'échelle pour A et B = 10 cm.

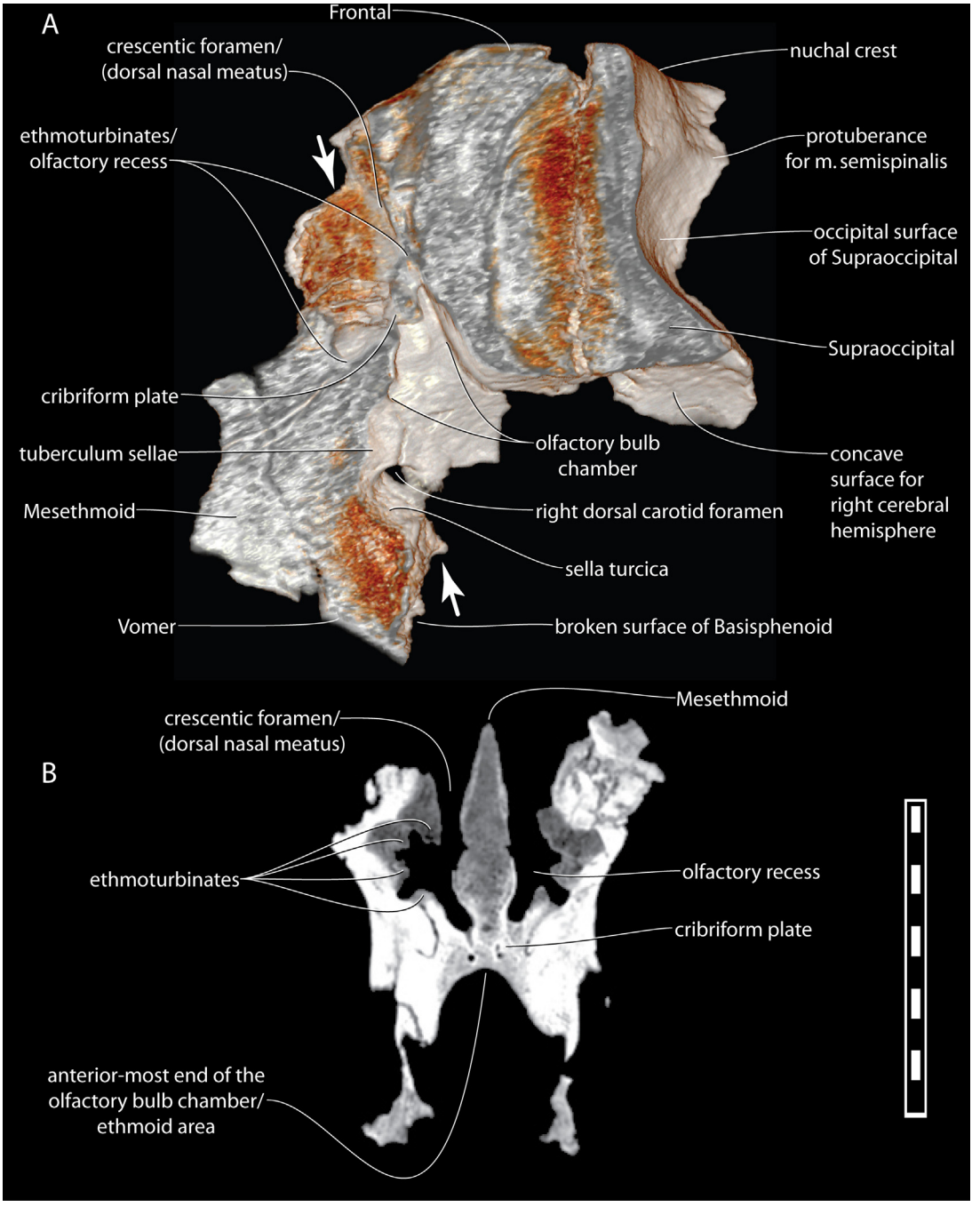


**Fig. 3.** A. Partial skull of CMM-V-2287, *Squalodon* sp., in parasagittal section (a to a' in Fig. 1C) showing the orientation and position of the right half of the olfactory bulb chamber and cribriform plate lying dorsal to the braincase. Anterior is to the left. Image based on CT scan images compiled and artificially colored in VuePAC®. B. Anterior view of a single CT scan image showing a subvertical transverse section through part of the olfactory apparatus of CMM-V-2287 at the position indicated by the two arrows in A and b and b' in Fig. 1C. At this position within the olfactory recesses, four ethmoturbinates extend into the right recess, whereas three are present in the left. Scale bar equals 10 cm.

**Fig. 3.** A. Portion de crâne de CMM-V-2287, *Squalodon* sp. en coupe parasagittale (selon la ligne a–a' de la Fig. 1C) montrant l'orientation et la position de la moitié droite de la chambre bulbaire olfactive et la plaque criblée au dos de la boîte crânienne. L'avant est vers la gauche. Images au scan CT compilées et artificiellement colorées par VuePAC®. B. Vue antérieure d'une unique image au scan CT montrant une section transverse subverticale de l'appareil olfactif de CMM-V-2287 à la position indiquée par les deux flèches en A et b et b' à la Fig. 1C. À cette position dans les cavités olfactives, quatre ethmoturbinaux se développent dans la cavité droite, alors qu'il y en a trois dans la cavité gauche. Barre d'échelle = 10 cm.

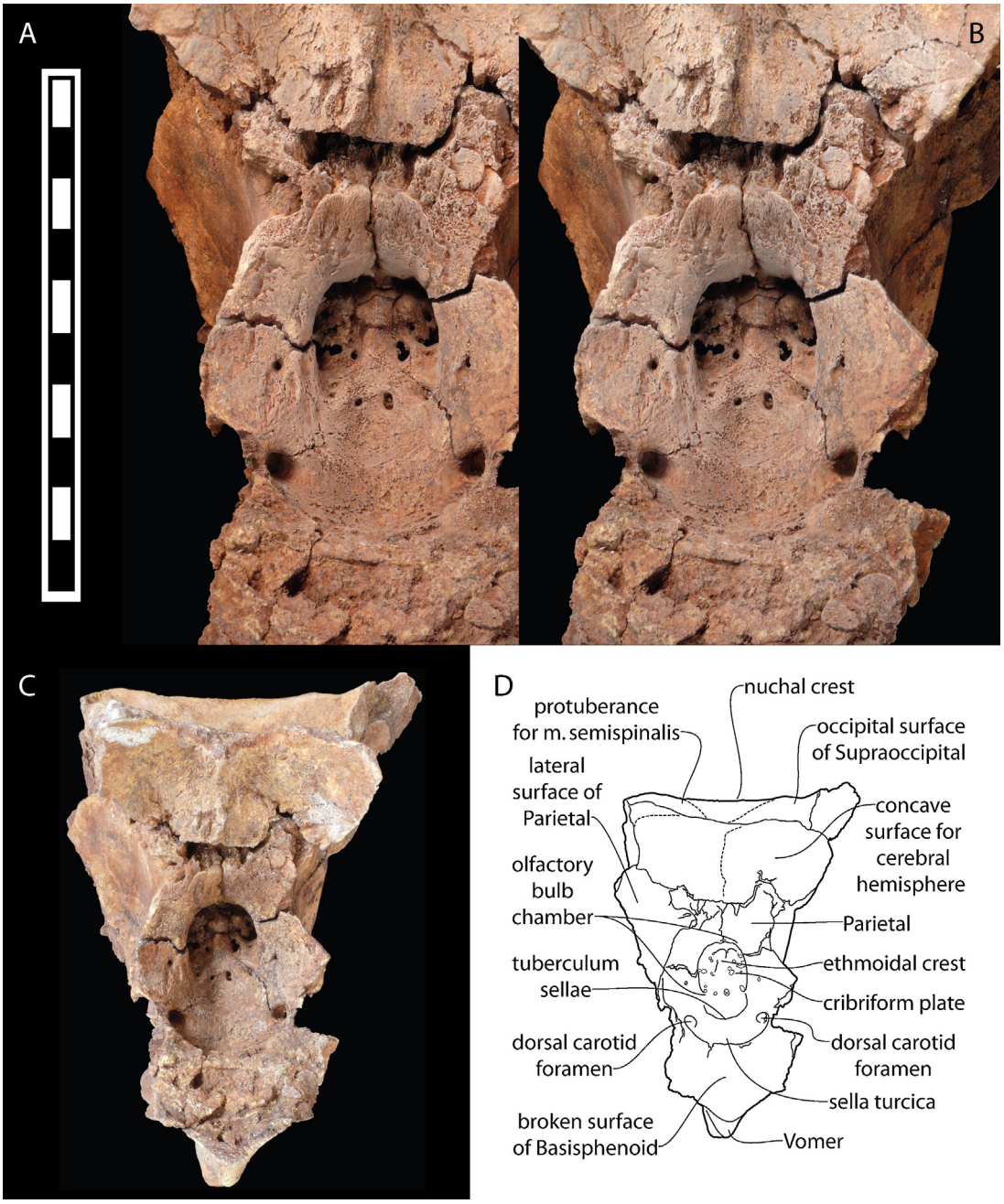


**Fig. 4.** A and B. Stereo pairs of a ventral/internal view of a broken skull of CMM-V-2287, *Squalodon* sp., showing part of the anterodorsal interior of the cranial cavity, olfactory bulb chamber, and cribriform plate. C. Ventral/internal view of all of the skull section shown in Figs. 2 and 3A and B. D. Interpretive line drawing showing the salient features of CMM-V-2287 shown in C. Scale bar for A and B equals 10 cm.
**Fig. 4.** A et B. Couple stéréoscopique en vue ventrale/interne d'un crâne brisé de CMM-V-2287, *Squalodon* sp., montrant une partie de l'intérieur de la cavité crânienne, de la chambre olfactive bulbaire et de la plaque criblée. C. Vue ventrale et interne du crâne représenté aux Fig. 2 et 3A et B. D. Dessin interprétatif au trait montrant les traits marquants de CMM-V-2287 figurés en C. Barre d'échelle = 10 cm.

axis of the skull (Figs. 3A and 4). The minimum diameter of the bulb chamber is about 29 mm, but the space increases somewhat in diameter dorsally around the perimeter of the cribriform plate. A conical protuberance (i.e., the ethmoidal crest) occupies the center of the olfactory bulb chamber. A smaller conical protuberance lies on either side of the ethmoidal crest (Fig. 4). Surrounding these are the many foramina that perforate the cribriform plate. The tuberculum sellae marks the anteroventral margin of the olfactory bulb chamber (Figs. 3A and 4).

CT scans of CMM-V-2287 permit visualization of the orientation of the olfactory bulb chamber. In Fig. 3A, CMM-V-2287 is seen in a parasagittal section close to the midline of the skull (Fig. 1C, a–a'). The supraoccipital forms a high

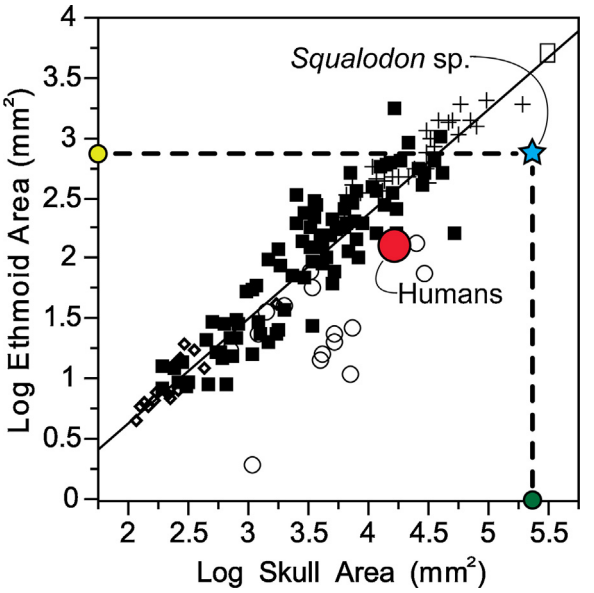


**Fig. 5.** Regression of log-transformed ethmoid bone area on skull area (both in $mm^2$) in a variety of mammals, from Pihlström et al. (2005) to which was added CMM-V-2287, *Squalodon* sp., represented by the bold blue 5-point star. The least-squares regression equation is log (ethmoid area) = −1.119 + 0.871 log (skull area) ($n$ = 150, $r^2$ = 0.815). The relationship is weakly but significantly negatively allometric (95% confidence interval of regression coefficient 0.821–0.919). Symbol coding: diamonds, bats; open circles, primates; crosses, artiodactyls. The large red circle and open rectangle show *Homo sapiens* and *Elephas maximus*, respectively. Complete data can be found in the Electronic Appendix accompanying Pihlström et al. (2005). For interpretation of references to color, see the online version of this article.

**Fig. 5.** Régression de la surface log-transformée de l'os ethmoïde sur la surface du crâne (les deux en $mm^2$), dans une grande variété de mammifères (Pihlström et al., 2005), à laquelle a été ajouté CMM-V-2287, *Squalodon* sp., représenté par l'étoile bleue à cinq pointes. L'équation de régression de moindre carré est : log (surface de l'ethmoïde) = −1,119 + 0,871 (surface du crâne) ($n$ = 150, $r^2$ = 0,815). La relation est faiblement, mais significativement, négativement allométrique (intervalle de confiance à 95 % du coefficient de régression 0,821–0,919). Signification des symboles : losanges : chauves-souris ; cercles blancs : primates ; croix : artiodactyles. Le grand cercle rouge et le rectangle représentent *Homo sapiens* et *Elephas maximus*, respectivement. Les données complètes peuvent être trouvées dans l'appendice accompagnant Pihlström et al. (2005). Pour l'interprétation des références aux couleurs, voir la version en ligne de cet article.

and robust vertical plate above the dorsally convex surface for the cerebral hemispheres. The thickness of the frontoparietal complex equals that of the supraoccipital with which they share a vertical suture. Passing anteriorly from the ventrally concave surface for the cerebral hemispheres, the olfactory tract turns sharply anterodorsally so that the olfactory bulb chamber, the cribriform plate, and the olfactory recesses were entirely dorsal to the braincase.

### 2.1. *Olfactory ability in* Squalodon *sp.*

Pihlström et al. (2005) found that in extant mammals, for which relevant data were available, the area of the perforated ethmoid bone (i.e., the cribriform plate) is directly proportional to both the area of the skull (Fig. 5) and the olfactory epithelium covering the ethmoturbinates (Fig. 6). In an attempt to quantify the olfactory ability of *Squalodon* sp., the area of the ethmoid (cribriform plate; i.e., Log ethmoid area in Figs. 5 and 6) was calculated and plotted on two graphs originally compiled by Pihlström et al. (2005). Additionally, the Log skull area (shown in Fig. 5) and the Log epithelium area (shown in Fig. 6) were also calculated for CMM-V-2287 (see below).

In mammals, the perforated part of the ethmoid bone approximates an oblate ellipsoid (Pihlström et al., 2005). Although the posteroventral surface of the perforate ethmoid (cribriform plate) in CMM-V-2287 is complex (Fig. 3), it more closely approximates the surface area of an ellipse, which area was calculated on the basis of dimensions taken from CT scans viewed in VuePAC®. The area enclosed by an ellipse is $\pi ab$, where $a$ and $b$ are one-half of the ellipse's major and minor axes, respectively.

Ethmoid area for CMM-V-2287: major axis = 37.7 mm (wide); minor axis = 26.0 mm.

Ethmoid area = $\pi ab$ = 3.14159 × 18.85 mm × 13.0 mm = 769.8 $mm^2$.

Log 769.8 = 2.88.

Log ethmoid area = 2.88; plotted in Figs. 5 and 6 (yellow dot in both figures).

To obtain mammalian skull area for the purpose of their analysis, Pihlström et al. (2005) multiplied condylobasal length by cranial base width. For cranial base width, Pihlström et al. (2005) measured the width of the basicranium, i.e., its width between the mastoid processes. In non-cetacean mammals, this dimension can be measured fairly unambiguously (Pihlström pers comm., Oct. 4, 2012). Cetaceans do not have a comparable mastoid process (Mead and Fordyce, 2009); therefore, a proxy width measurement was taken as the distance between the lateral extremities of the exoccipitals. In CMM-V-2287, skull width was obtained by doubling the measurement from the left half of the skull. The basicranium in squalodontids is symmetrical therefore a high degree of confidence can be placed in this computed dimension. Unfortunately, because CMM-V-2287 is broken into so many pieces, it has not yet been possible to completely reassemble the skull to obtain an accurate condylobasal length. Consequently, skull length for CMM-V-2287 was calculated from the proportions of USNM 183023 and USNM 424070, the type and paratype specimens of *S. whitmorei* respectively (Fig. 1A). In CMM-V-2287, condylobasal length was calculated by scaling down condylobasal length in USNM 183023 and USNM 424070 to match the cranial width in CMM-V-2287.

In CMM-V-2287, skull area = condylobasal length × width of skull across exoccipitals.

Skull area = 900 mm × 316 mm = 284,400 $mm^2$.

Log 284,400 = 5.45.

Log skull area = 5.45; plotted in Fig. 5 (green dot).

If the proportions of *S. calvertensis* (Fig. 1B) are used to calculate the condylobasal length in CMM-V-2287, the resulting Log skull area in Fig. 5 would move from 5.45 to approximately 5.50; an insignificant shift vis-à-vis the conclusions to which these calculations point.

Furthermore, the surface area of the ethmoturbinates within the olfactory recesses, which in life is presumed to have been covered with olfactory epithelium, was calculated from CT images using Mimics®. The olfactory recesses

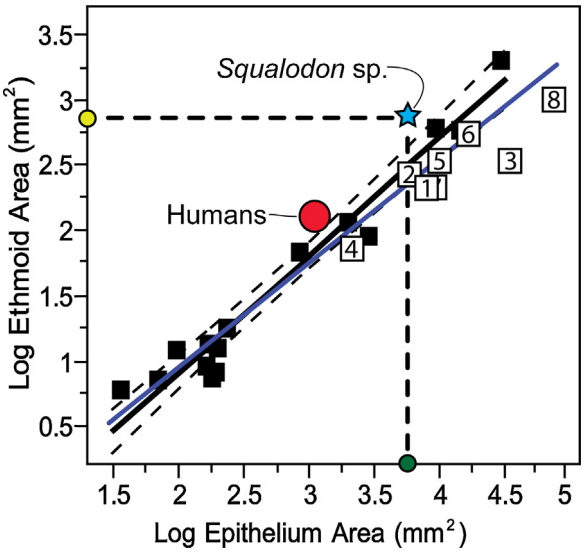


**Fig. 6.** Regression of log-transformed ethmoid bone area on olfactory epithelium area (both in $mm^2$); data and graph from Pihlström et al. (2005, table 1 and modified fig. 2). The least-squares regression equation from Pihlström et al. (2005, black lines both solid and dashed) is log (ethmoid area) = –0.883 + 0.900 log (epithelial area) ($n$ = 16, $r^2$ = 0.953). Dashed lines adjacent to the regression line show 95% confidence limits of their least-squares fit. The large red circle shows *Homo sapiens*. Nine additional data points have been added to Pihlström et al. (2005). They include: the blue 5-point star representing CMM-V-2287, *Squalodon* sp., and the numbered open squares representing: (1) striped skunk, *Mephitis mephitis* (log male olfactory surface areas = 3.825, log ethmoid area = 2.371); (2) sea otter, *Enhydra lutris* (log male olfactory surface areas = 3.791, log ethmoid area = 2.435); (3) wolverine, *Gulo gulo* (log male olfactory surface areas = 4.554, log ethmoid area = 2.544); (4) American mink, *Neovison (Mustela) vison* (log male olfactory surface areas = 3.372, log ethmoid area = 1.843); (5) American badger, *Taxidea taxus* (log male olfactory surface areas = 4.065, log ethmoid area = 2.589); (6) California sea lion, *Zalophus californianus* (log male olfactory surface areas = 4.243, log ethmoid area = 2.738); (7) raccoon, *Procyon lotor*, mostly hidden by box number 1 (log male olfactory surface areas = 3.986, log ethmoid area = 2.394); and (8) brown bear, *Ursus arctos* (log male olfactory surface areas = 4.915, log ethmoid area = 3.002). The eight numbered data points were compiled from log male olfactory surface areas from Van Valkenburgh et al. (2011, table 1, Olf SA column) and the average log ethmoid areas from Pihlström et al. (2005, table 1) for those species that occur in both studies. The new log-transformed regression line using all 25 data points is log (ethmoid area) = –0.627 + 0.782 log (epithelial area) ($n$ = 25, $r^2$ = 0.919). For interpretation of references to color, see the online version of this article.

**Fig. 6.** Régression de la surface log-transformée de l'os ethmoïde sur celle de l'épithélium olfactif (toutes les deux en $mm^2$) ; les données et le graphique sont de Pihlström et al. (2005, tableau 1 et fig. 2 modifiée). L'équation de régression de moindre carré, selon Pihlström et al. (2005, lignes noires, pleines et tiretées) est : log (surface de l'ethmoïde) = –0,883 + 0,900 log (surface épithéliale) ($n$ = 16, $r^2$ = 0,953). Les lignes tiretées adjacentes à la ligne de régression montrent les limites de confiance à 95 % de leur ajustement par moindres carrés. Le grand cercle rouge représente *Homo sapiens*. Neuf données additionnelles ont été ajoutées à celles de Pihlström et al. (2005). Elles comportent : l'étoile bleue à cinq pointes représentant CMM-V-2287, *Squalodon* sp., et les carrés blancs numérotés correspondant à : (1) sconse tigré, *Mephitis mephitis* (log surfaces olfactives de mâle = 3,825, log surface de l'ethmoïde = 2,371) ; (2) phoque, *Euhydra lutris* (log surfaces olfactives de mâle = 3,791, log surface de l'ethmoïde = 2,435) ; (3) wolverine, *Gulo gulo* (log surfaces olfactives de mâle = 4,554, log surface de l'ethmoïde = 2,544) ; (4) vison, *Neovison (Mustela) vison* (log surfaces olfactives de mâle = 3,372, log surface de l'ethmoïde = 1,843) ; (5) blaireau américain, *Taxidea taxus* (log surfaces olfactives de mâle = 4,065, log surface de l'ethmoïde = 2,589) ; (6) otarie californienne, *Zalophus californianus* (log surfaces olfactives de mâle = 4,243, log surface de l'ethmoïde = 2,738) ; (7) raton-laveur, *Procyon lotor*, en grande partie caché par la boîte 1 (log surfaces olfactives de mâle = 3,986, log surface de l'ethmoïde = 2,394) ; et (8) ours brun, *Ursus arctos* (surfaces olfactives de mâle = 4,915, log surface de l'ethmoïde = 3,002). Ces huit groupes de données numérotées ont été compilés à partir des logs surfaces olfactives de mâle de Van Valkenburgh et al. (2011, tableau 1, colonne Olf SA) et de la moyenne des log surfaces de l'ethmoïde de Pihlström et al. (2005, tableau 1) pour les espèces observées dans les deux types d'étude. La nouvelle ligne de régression log-transformée utilisant les 25 données est log (surface de l'ethmoïde) = –0,627 + 0,787 log (surface épithéliale) ($n$ = 25, $r^2$ = 0,919). Pour l'interprétation des références aux couleurs, voir la version en ligne de cet article.

were digitally partitioned in a vertical transverse plane into seven, 5-mm-wide sections (Fig. 2D). Working in Mimics®, the length of the convoluted leading edge of each section was measured in millimeters. The surface area for each section of the nasal/olfactory recess was then obtained by multiplying the aforementioned leading-edge length by 5 mm. Surface areas were calculated for both right and left olfactory recesses and then combined for the total area covered by olfactory epithelium. If olfactory epithelium extended beyond the ethmoturbinate-bearing recesses at the base of the crescentic foramina, then the surface area computed here would represent an underestimate. The converse could also be true.

Olfactory epithelium area within the olfactory recesses = 5367 $mm^2$ (2711 $mm^2$ for the right side; 2656 $mm^2$ from the left side).

Log 5367 = 3.72.

Log epithelium area = 3.72; plotted in Fig. 6 (green dot).

Observations drawn from the Log ethmoid area vs. Log skull area graph (Fig. 5):

- the Log ethmoid area (2.88) (i.e., the area of the cribriform plate) in CMM-V-2287, *Squalodon* sp., is large as compared to most other mammals (as measured by Pihlström et al., 2005, appendix 1);

- the ethmoid area is comparable to that of most extant artiodactyls; a group indicated by crosses in Fig. 5;
- the ethmoid area in CMM-V-2287 is 5.8 times that of humans [769.8 $mm^2$ in *Squalodon* sp. vs. 132 $mm^2$ in *Homo sapiens* (Pihlström et al., 2005, table 1)];
- CMM-V-2287 is the only cetacean in which the area of the cribriform plate has been measured. Compared to its Log skull area, CMM-V-2287 has a smaller Log ethmoid area than would be expected if it was more like mammals that approximate the best-fit line. Perhaps it is important to point out that the rostrum in squalodontids is proportionately longer than in terrestrial mammals. Everything else being equal, an elongate rostrum would overstate/bias the size of Log skull area, pulling long-snouted odontocetes (like squalodontids, eurhinodelphinids, and platanistids which retain a measurable ethmoid area) away from the best-fit line, exaggerating the reduction in their olfactory ability. However, even if the condylobasal length is cut in half, i.e., reduced from 900 mm to 450 mm, skull area = 450 mm × 316 mm = 142,200 $mm^2$, Log 142,200 = 5.15. This would still place *Squalodon* sp. below the best-fit line; comparable to the distance from the line to which humans are removed;
- in terms of the ratio – Log ethmoid area to Log skull area, CMM-V-2287 falls below the best-fit line, comparable to the four other lowest ratios: those of two monkeys (the guereza and the red-handed tamarin), the orangutan, and the dugong (the black square to the right of the large red human circle) (Pihlström et al., 2005). Mammals with ratios that fall well below the line have olfactory abilities inferior to mammals with comparable skull areas that plot above the best-fit line. In Fig. 5, open circles denote primates; a group within which the anthropoids have a generally reduced olfactory ability (Rouquier et al., 2000);
- all, but possibly the most archaic, Odontoceti would be expected to plot below the best-fit line; a reflection of the long-term evolutionary reduction in the size of their olfactory apparatus, see below. No post-Langhian odontocete is known to have a larger olfactory apparatus than that of CMM-V-2287;
- if extant adult odontocetes were added to this graph, most would plot close to or along the Log skull area axis (i.e., the *x*-axis), having no significant development of olfactory bulb chambers. O. Lambert (pers. comm., Feb. 2013) brought to the author's attention two ziphiids (*Mesoplodon grayi* [USNM 49880] and *Tasmacetus shepherdi* [USNM 484878]) in which there exists a bony fold or pocket in the ethmoid at the location of the olfactory recess in *Squalodon*, in and surrounding which are numerous perforations that one would not hesitate to refer to as a cribriform plate if significant olfactory bulb chambers were present within the cranial cavity. *Physeter macrocephalus* Linnaeus, 1758 is the largest extant mammal in which there are no olfactory bulb chambers [extant baleen whales retain a functional olfactory apparatus and olfactory bulb chambers (Godfrey et al., 2013; Hoch, 2000; Thewissen et al., 2011)]. The Log skull area in *P. macrocephalus*, USNM 301634, is a very impressive 7.04 (5207 mm condylobasal length × 2146 mm, skull width = 11,174,222 $mm^2$. Log 11,174,222 = 7.04; off the chart in Fig. 5) and yet its Log ethmoid area seems to be zero.

Observations drawn from the Log ethmoid area/Log epithelium area graph (Fig. 6):

- nine additional taxa were added to Pihlström et al. (2005, fig. 2); CMM-V-2287 (*Squalodon* sp.) the bold blue 5-point star, and the eight numbered open squares that represent aquatic and terrestrial carnivorans compiled from log male olfactory surface areas from Van Valkenburgh et al. (2011, table 1, Olf SA column) and log ethmoid areas from Pihlström et al. (2005, supplementary Electronic Appendix, available at http://dx.doi.org/10.1098/rspb.2004.2993 or via http://www.journals.royalsoc.ac.uk) for those species that occur in both studies. All of the carnivorans (terrestrial and aquatic) from the Van Valkenburgh et al. (2011) study lie below the original solid black best-fit line in Fig. 6, suggesting above average olfactory ability as compared to the other mammals that Pihlström et al. (2005) used to generate the original graph. Using all 25 data points, the new log-transformed regression line (in blue) is: log (ethmoid area) = –0.627 + 0.782 log (epithelial area) ($n = 25$, $r^2 = 0.919$). The lower $r^2$ value, from 0.953 to 0.919, reflects greater scatter distally about the best-fit line contributed to no doubt by disparate entries like *Squalodon* sp. and the wolverine, *Gulo gulo*, which are approximately equally far removed above and below the new blue regression line respectively. Although the two aquatic carnivorans (sea otter, *Enhydra lutris* [Box #2] and California sea lion, *Zalophus californianus* [Box #6]) that Van Valkenburgh et al. (2011) illustrate to have reduced olfactory turbinates as compared with terrestrial carnivorans, they give no indication relative to the best-fit line of being deficient in olfactory ability;
- both *Squalodon* sp. and humans lie above the best-fit line. This means that in both, the surface area of their olfactory epithelium is smaller relative to their ethmoid area as compared to most mammals in which these areas have been measured;
- the surface area of the olfactory epithelium in CMM-V-2287 is 4.77 times larger than in humans and nearly double that of the cat (CMM-V-2287 = 5367 $mm^2$; humans = 1125 $mm^2$; *Felis catus* = 2791 $mm^2$). Pihlström et al. (2005) found that olfactory sensitivity increased with an increase in organ size; consequently, CMM-V-2287 gives every indication that its olfactory ability exceeded that of humans and domestic cats;
- furthermore, in CMM-V-2287, the area of the cribriform plate (i.e. the ethmoid area) is greater than that of a roe deer or a dog (*Squalodon* sp. = 769.8 $mm^2$; roe deer, *Capreolus capreolus* = 588 $mm^2$; German shepherd, *Canis familiaris* = 578 $mm^2$) (Pihlström et al., 2005, table 1);
- however, as compared to the surface area of their ethmoturbinates, the roe deer and dog nearly double and triple respectively the surface area of that of *Squalodon* sp. (CMM-V-2287 = 5367 $mm^2$; roe deer = 9000 $mm^2$; dog = 13,900 $mm^2$). Therefore, it is probably reasonable

to conclude that the olfactory ability of *Squalodon* sp. was far exceeded by that of the roe deer and dog;
- CMM-V-2287 shows that well into the Miocene, some odontocetes probably retained a reasonably well-developed sense of smell;
- the area of the mammalian olfactory epithelium is typically circa 16 times larger than the ethmoid area (Pihlström et al., 2005). However, in CMM-V-2287, although the area of the olfactory epithelium was relatively large, it was only about seven times larger than its ethmoid area, less than half the epithelium area in typical mammals;
- it is expected that most or all extant adult odontocetes could not be graphed, having neither a measurable ethmoid nor olfactory epithelium area.

## 3. Discussion

The olfactory apparatus is poorly known in archaic odontocetes and has only been described in two unnamed Oligocene odontocetes (Fordyce, 2002; USNM 299482, fig. 5E; Hoch, 2000, figs. 6 and 7) and the Early Miocene prosqualodontid *Prosqualodon davidi* (Flynn, 1948). Hoch (2000) provides the most detailed account for an unnamed Latest Oligocene platanistoid odontocete from Denmark, MGUH VP 3338. It shares the following similarities and differences with the one described herein. Both present crescentic foramina (dorsal nasal meatuses), although in the Oligocene platanistoid, the crescentic foramina (which Hoch (2000) refers to as "laterally concave apertures") are much reduced as compared to those of CMM-V-2287, *Squalodon* sp. The present author would consider the laterally concave apertures in MGUH VP 3338 to be amongst the smallest remnants of the dorsal nasal meatuses known within Cetacea, and despite its Latest Oligocene age derived in every way relative to the configuration present in CMM-V-2287. Both exhibit three low ethmoturbinates, although four are present on the right side in CMM-V-2287. The long axis of the ethmoturbinates in CMM-V-2287 is horizontal, whereas in MGUH VP 3338, they appear to be subvertical; presumably the result of its olfactory recesses having been further reduced dorsoventrally and compressed anteroposteriorly. A larger number of ethmoturbinates having a mostly horizontal long axis are considered primitive over the condition exhibited by MGUH VP 3338. The posteroventral surface of the crescentic foramina in both comprises the area occupied by the perforate cribriform plate. Both odontocetes are considered to have had olfactory ability, although the sensitivity in CMM-V-2287, *Squalodon* sp., was probably greater because of its larger size.

Much of the olfactory apparatus in CMM-V-2287 is also directly comparable to that in archaeocetes and the extant minke whale (*Balaenoptera acutorostrata*) (Godfrey et al., 2013). In CMM-V-2287, the internal nares were unobstructed by turbinates. As in all cetaceans, they have no respiratory turbinates within their nasal cavity, allowing for the rapid exchange of a large volume of air when surfacing (Reidenberg and Laitman, 2008). (Exactly when in the course of cetacean evolution were respiratory turbinates completely lost remains unknown. Clearly, they were lost long before ethmoturbinates vanished). To achieve an unobstructed nasal cavity and retain a sense of smell, the olfactory recesses in CMM-V-2287 comprise a diverticulum or niche posterior to the main open airway of the internal nares. Instead of the dorsal nasal meatuses presenting as elongate subhorizontal troughs as they do in archaeocetes and the extant minke whale, in archaic odontocetes, including *Squalodon* sp. with fully telescoped skulls, the troughs have been shortened dramatically to form crescentic foramina.

Some mammals, perhaps including archaeocetes and the extant minke whale, have, to varying degrees, separate olfactory and respiratory airflows through the nasal cavity. Separation is achieved in large part through the preferential movement of air along different paths within the nasal cavity. Craven et al. (2010) found that during inspiration in dogs, most of the air entering the olfactory ethmoturbinates arrives along the dorsal nasal meatus. The remaining respiratory airflow is directed more ventrally within the nasal cavity on its way to the lungs. In CMM-V-2287, it is not known to what extent if any soft tissue and accessory nasal air sacs associated with its ability to echolocate separated airflows between its internal nares and its olfactory recesses. Osteologically, in CMM-V-2287, the crescentic foramina are open anteriorly throughout their height and in life air could have communicated freely between the foramina and the internal nares in the absence of intervening soft tissue. Inhaled air flowing along the crescentic foramina would have descended to the posterior reaches of each olfactory recess, passed forward along the length of the ethmoturbinates, and then in the absence of obstructing soft tissues, continued forward up and over the anterior lip of the olfactory recess to rejoin the majority of the air streaming ventrally through the internal nares towards the lungs. It is not known whether exhaled air bypassed the olfactory recesses in *Squalodon* to create a unidirectional airflow within these recesses.

The Odontoceti-Mysticeti split occurred between 33–37 MYA, Xiong et al. (2009) dated it at 33.7 MYA; Chen et al. (2011), Zhou et al. (2011), and Hassanin et al. (2012) 34.4 MYA; Steeman et al. (2009) 36 MYA; and McGowen et al. (2009) 36.4 MYA. Since then, these two crown-groups have taken different evolutionary paths when it comes to the way in which they capture prey. Most baleen whales have become increasingly specialized in bulk-feeding (Goldbogen, 2010; Pivorunas, 1979; Pyenson et al., 2012) whereas toothed whales developed echolocation which is used, among other things, to locate prey, consuming them singly (Balance, 2009; Cranford, 1988; Uhen, 2010). At a minimum, olfaction appears to contribute to the success of bulk-feeding mysticetes, whereas it does not seem to play any part in improving the predatory ability of extant odontocetes.

Extant mysticetes that have been studied in this regard are now known to have a functional olfactory system (Edinger, 1955; Godfrey et al., 2013; Hoch, 2000; Kishida and Thewissen, 2012; Oelschläger and Oelschläger, 2009; Thewissen et al., 2011). Krill-eating mysticetes apparently rely on olfaction to find their food (Cave, 1988; Hoch, 2000; Oelschläger and Oelschläger, 2009; Purves and Pilleri, 1983; Thewissen et al., 2011), sniffing by way of short inhalations, distinct from their powerful respirations

(Hoch, 2000), perhaps doing so to track the distinctive odor so characteristic of these crustaceans (Thewissen et al., 2011). Krill and phytoplankton both produce dimethyl sulfide (DMS), which when detected in significant atmospheric concentrations by marine predators would hold the promise of a foraging feast (Nevitt, 1999; Van Valkenburgh et al., 2011). Several non-cetacean vertebrates hone in on DMS as a foraging cue; krill-feeding procellariiform birds (Nevitt, 1999; Nevitt and Haberman, 2003; Nevitt et al., 1995) and some seals (Kowalewsky et al., 2006).

Echolocation (also known as biosonar) is an active sonar mechanism whereby odontocetes produce sound, the reflections of which allow them to create a soundscape of their underwater world (Cranford, 1988; Schevill and McBride, 1956; Whitlow, 2009 and the references therein). Baleen whales do not echolocate although they do vocalize to synchronize biological and behavioral activities (Dudzinski et al., 2009). It would seem that, at least in part if not wholly, the evolution of this ability to "see" with sound in odontocetes contributed more than any other factor to a reduction and eventual apparent loss of the odontocete sense of smell. An increase in the size and sophistication of the sound-production mechanism (the phonic lips and associated facial air sacs), the melon, coupled with the concomitant backwards movement of the nostrils to the top of their head, seemingly put the squeeze on their sense of smell, sandwiched between the brain and the enlarging components of this new and highly prized evolutionary discovery; the ability to echolocate.

Most mammals rely heavily upon olfaction to find food, recognize conspecifics, establish and maintain social interactions, find fertile mates, detect potential threats, and orient themselves (Rowe et al., 2005; Stoddart, 1980a, 1980b). Anosmatic extant odontocetes can hardly be said to be inept (or completely lacking) in any of the aforementioned aspects of life as compared to other mammals in which olfaction is so critical to their survival. Olfactory cues that had hitherto contributed to successful predation and social/parental/sexual interactions in archaeocetes were "abandoned" in odontocetes in favor of biosonar that rendered the chemical-cue sensory input system redundant/obsolete. Evidently, during the course of odontocete evolution, what cognitive/sensory information was lost as their osmatic ability waned was replaced, at least in part, or entirely and possibly then some by biosonar (i.e. acoustic cues sent and received replaced and probably surpassed the effectiveness of gathering chemical/olfactory cues in an aquatic environment). Within the Odontoceti, one sensory system (sound generation/hearing) eclipsed another (olfaction), providing the same kind of environmental-interactive information (to thrive and maintain social bonds), derived from a completely different mode of information generation and collection.

It is not yet possible to know to what degree *Squalodon* sp., or other Miocene toothed whales employed their sense of smell. In most, it seems to have been of lesser importance than their ability to echolocate. Perhaps both senses worked together; overlapping and/or complimenting each other. What is known is that during the Miocene, most odontocetes variously lost the bony structures associated with an ability to smell.

## Acknowledgments

During the summer of 1982, I spent a month in Garnett, Kansas – member of a field party led by Dr. Robert Reisz. That field experience was amazing for several reasons, but the discovery of small reptilian footprints at many levels within the quarry was transformative in terms of how a then Young-Earth Creationist saw the world. Robert, thank you for those memories and then for some years later taking me on as a Postdoctoral Fellow. I hope you enjoy this contribution on a highly derived synapsid with a reduced olfactory apparatus!

I wish to express my thanks to Michel Laurin for the invitation to contribute to this volume honoring Robert.

CMM-V-2287 was discovered by Paul Murdoch. He, P. Fink, S. Werts, W. Counterman, and the author collected what remained of the skull. E. Woo very kindly allowed us to quarry on her cliff-front property and then donated the find to the Calvert Marine Museum; many thanks. H. Pihlström (University of Helsinki) provided digital versions of the graphs that appear in his 2005 publication. Both he and The Royal Society are gratefully acknowledged for permission to modify and then republish Figs. 5 and 6. J. Nance (CMM) was instrumental in generating the Mimics® image used in Fig. 2D. J. Siewerdsen, W. Zbijewski, and A. Muhit [The I-STAR Laboratory (www.jhu.edu/istar), Johns Hopkins University] patiently assisted with the use of Mimics® and VuePAC® in J. Siewerdsen's lab; thank you all. N. Pyenson, C. Potter, J. Ososky, and D. Bohaska (all USNM) encouraged use of the fossil and extant odontocete collections housed in the United States National Museum of Natural History, the Smithsonian Institution. J. Pojeta (USNM) provided liberal access to his lab where CMM-V-2287 was whitened with sublimed ammonium chloride; many thanks John for your ongoing generosity. K. Godfrey and M. Godfrey helped with arithmetic calculations.

Valuable critiques by O. Lambert (Royal Belgian Institute of Natural Sciences) and one anonymous reviewer substantially improved upon my initial submission; many thanks for your efforts on my behalf.

This publication was made possible with funding from the Board of Calvert County Commissioners, the citizens of Calvert County, MD, and the Clarissa and Lincoln Dryden Endowment for Paleontology at the Calvert Marine Museum.

## References

Balance, L.T., 2009. Cetacean ecology. In: Perrin, W.F., Würsig, B., Thewissen, J.G.M. (Eds.), Encyclopedia of Marine Mammals, second ed. Elsevier, Amsterdam, Netherlands, pp. 196–201.

Breathnach, A.S., 1960. The cetacean central nervous system. Biol. Rev. Camb. Philos. Soc. 35, 187–230.

Cave, A.J.E., 1988. Note on olfactory activity in mysticetes. J. Zool. London 214, 307–311.

Chen, Z., Xu, S., Zhou, K., Yang, G., 2011. Whale phylogeny and rapid radiation events revealed using novel retroposed elements and their flanking sequences. BMC Evol. Biol. 11, 314.

Cranford, T.W., 1988. The anatomy of acoustic structures in the spinner dolphin forehead as shown by X-ray computed tomography and computer graphics. In: Nachtigall, P.E., Moore, P.W.B. (Eds.), Animal Sonar: Processes and Performance. Plenum Press, New York, pp. 67–77.

Craven, B.A., Paterson, E.G., Settles, G.S., 2010. The fluid dynamics of canine olfaction: unique nasal airflow patterns as an explanation of macrosmia. J. Roy. Soc. Interface 7, 933–943.
Dooley Jr., A.C., 2003. A review of the eastern North American Squalodontidae (Mammalia, Cetacea). Jeffersoniana 11, 1–26.
Dooley Jr., A.C., 2005. A new species of *Squalodon* (Mammalia, Cetacea) from the Middle Miocene of eastern North America. Va. Mus. Nat. Hist. Mem. 8, 43.
Dudzinski, K.M., Thomas, J.A., Gregg, J.D., 2009. Communication in marine mammals. In: Perrin, W.F., Würsig, B., Thewissen, J.G.M. (Eds.), Encyclopedia of Marine Mammals, second ed. Elsevier, Amsterdam, Netherlands, pp. 260–269.
Edinger, T., 1955. Hearing and smell in cetacean history. Monatssc. Psychiatr. Neurol. 129, 37–58.
Flynn, T.T., 1948. Description of *Prosqualodon davidi* Flynn, a fossil cetacean from Tasmania. Trans. Zool. Soc. Lond. 26, 153–197.
Fordyce, R.E., 2002. *Simocetus rayi* (Odontoceti: Simocetidae, New Family): a bizarre new archaic Oligocene dolphin from the eastern North Pacific. Smithson. Contrib. Paleobiol. 93, 185–222.
Fordyce, R.E., 2009. Cetacean fossil record. In: Perrin, W.F., Würsig, B., Thewissen, J.G.M. (Eds.), Encyclopedia of Marine Mammals, second ed. Elsevier, Amsterdam, Netherlands, pp. 207–215.
Godfrey, S.J., Geisler, J., Fitzgerald, E.M.G., 2013. On the olfactory anatomy in an archaic whale (Protocetidae, Cetacea) and the minke whale *Balaenoptera acutorostrata* (Balaenopteridae, Cetacea). Anat. Rec. 296, 257–272.
Goldbogen, J.A., 2010. The ultimate mouthful: lunge feeding in rorqual whales. Am. Scientist 98, 124–131.
Gottfried, M.D., Bohaska, D.J., Whitmore Jr., F.C., 1994. Miocene cetaceans of the Chesapeake Group. In: Berta A., Deméré, T.A. (Eds.), Contributions in marine mammal paleontology honoring Frank C. Whitmore, Jr. Proc. San Diego Soc. Nat. Hist. 29, pp. 229–238.
Hassanin, A., Delsuc, F., Ropiquet, A., Hammer, C., Jansen van Vuuren, B., Matthee, C., Ruiz-Garcia, M., Catzeflis, F., Areskoug, V., Nguyen, T.T., Couloux, A., 2012. Pattern and timing of diversification of Cetartiodactyla (Mammalia, Laurasiatheria), as revealed by a comprehensive analysis of mitochondrial genomes. C. R. Biologies 335, 32–50.
Hoch, E., 2000. Olfaction in whales: evidence from a young odontocete of the Late Oligocene North Sea. Hist. Biol. 14, 67–89.
Kellogg, R., 1923. Description of two squalodonts recently discovered in the Calvert Cliffs, Maryland; and notes on the sharktoothed cetaceans. Proc. U. S. Nat. Mus. 62, Art. 16.
Kishida, T., Thewissen, J.G.M., 2012. Evolutionary changes of the importance of olfaction in cetaceans based on the olfactory marker protein gene. Gene 492, 349–353.
Kishida, T., Kubota, S., Shirayama, Y., Fukami, H., 2007. The olfactory receptor gene repertoires in secondary-adapted marine vertebrates: evidence for reduction of the functional proportions in cetaceans. Biol. Lett. 3, 428–430.
Kowalewsky, S., Dambach, M., Mauck, B., Dehnhardt, G., 2006. High olfactory sensitivity for dimethyl sulphide in harbour seals. Biol. Lett. 2, 106–109.
McGowen, M.R., Clark, C., Gatesy, J., 2008. The vestigial olfactory receptor subgenome of odontocete whales: phylogenetic congruence between gene-tree reconciliation and supermatrix methods. Syst. Biol. 57, 574–590.
McGowen, M.R., Spaulding, M., Gatesy, J., 2009. Divergence date estimation and a comprehensive molecular tree of extant cetaceans. Mol. Phylogenet. Evol. 53, 891–906.
Mead, J.G., Fordyce, R.E., 2009. The therian skull: a lexicon with emphasis on the odontocetes. Smithson. Contrib. Zool. 627, 1–249.
Nevitt, G.A., 1999. Olfactory foraging in Antarctic seabirds: a species-specific attraction to krill odors. Mar. Ecol. Prog. Ser. 177, 235–241.
Nevitt, G.A., Haberman, K., 2003. Behavioral attraction of Leach's storm-petrels (*Oceanodroma leucorrhoa*) to dimethyl sulfide. J. Exp. Biol. 206, 1497–1501.
Nevitt, G.A., Veit, R.R., Kareiva, P., 1995. Dimethyl sulphide as a foraging cue for Antarctic procellariiform seabirds. Nature 376, 680–682.
Oelschläger, H.A., 1992. Development of the olfactory and terminalis systems in whales and dolphins. In: Doty, R.L., Müller-Schwarze, D. (Eds.), Chemical Signals in Vertebrates VI. Plenum Press, New York, pp. 141–147.
Oelschläger, H.A., Oelschläger, J.S., 2009. Brain. In: Perrin, W.F., Würsig, B., Thewissen, J.G.M. (Eds.), Encyclopedia of Marine Mammals, second ed. Elsevier, Amsterdam, Netherlands, pp. 134–149.
Pihlström, H., Fortelius, M., Hemilä, S., Forsman, R., Reuter, T., 2005. Scaling of mammalian ethmoid bones can predict olfactory organ size and performance. Proc. Roy. Soc. B 272 (1566), 957–962.
Pivorunas, A., 1979. Feeding mechanisms of baleen whales. Am. Sci. 67, 432–440.
Purves, P.E., Pilleri, G.E., 1983. Echolocation in Whales and Dolphins. Academic Press, London.
Pyenson, N.D., Goldbogen, J.A., Vogl, A.W., Szathmary, G., Drake, R.L., Shadwick, R.E., 2012. Discovery of a sensory organ that coordinates lunge feeding in rorqual whales. Nature 485, 498–501.
Reidenberg, J.S., Laitman, J.T., 2008. Sisters of the sinuses: cetacean air sacs. Anat. Rec. 291, 1389–1396.
Rothausen, K., 1968. Die systematische Stellung der europäischen Squalodontidae (Odontoceti, Mamm.). Palaontol. Z. 42, 83–104.
Rouquier, S., Blancher, A., Giorgi, D., 2000. The olfactory receptor gene repertoire in primates and mouse: evidence for reduction of the functional fraction in primates. Proc. Natl. Acad. Sci. U S A 97, 2870–2874.
Rowe, T., Eiting, B., Thomas, P., Macrini, T.E., Ketcham, R.A., 2005. Organization of the Olfactory and Respiratory Skeleton in the Nose of the Gray Short-Tailed Opossum *Monodelphis domestica*. J. Mammal. Evol. 12 (3/4), 303–336.
Schevill, W.E., McBride, A.F., 1956. Evidence for echolocation by cetaceans. Deep Sea Res. 3, 153–154.
Sisson, S., Grossman, J.D., 1953. The Anatomy of the Domestic Animals, fourth ed. W.B. Saunders Company, Philadelphia, PA.
Steeman, M.E., Hebsgaard, M.B., Fordyce, R.E., Ho, S.Y.W., Rabosky, D.L., Nielsen, R., Rahbek, C., Glenner, H., Sørensen, M.V., Willerslev, E., 2009. Radiation of extant cetaceans driven by restructuring of the oceans. Syst. Biol. 58, 573–585.
Stoddart, D.M., 1980a. Olfaction in Mammals. Zoological Society of London, Symposium 45. Academic Press, London.
Stoddart, D.M., 1980b. The Ecology of Vertebrate Olfaction. Chapman and Hall, London.
Thewissen, J.G.M., George, J., Rosa, C., Kishida, T., 2011. Olfaction and brain size in the bowhead whale (*Balaena mysticetus*). Mar. Mammal Sci. 27, 282–294.
Uhen, M.D., 2010. The origin(s) of whales. Annu. Rev. Earth Planet. Sci. 38, 189–219.
Van Valkenburgh, B., Curtis, A., Samuels, J.X., Bird, D., Fulkerson, B., Meachen-Samuels, J., Slater, G.J., 2011. Aquatic adaptations in the nose of carnivorans: evidence from the turbinates. J. Anat. 218, 298–310.
Whitlow, W.L., 2009. Echolocation. In: Perrin, W.F., Würsig, B., Thewissen, J.G.M. (Eds.), Encyclopedia of Marine Mammals, second ed. Elsevier, Amsterdam, Netherlands, pp. 348–357.
Xiong, Y., Brandley, M.C., Xu, S., Zhou, K., Yang, G., 2009. Seven new dolphin mitochondrial genomes and a time-calibrated phylogeny of whales. BMC Evol. Biol. 9, 20.
Zhou, X., Xu, S., Yang, Y., Zhou, K., Yang, G., 2011. Phylogenomic analyses and improved resolution of Cetartiodactyla. Mol. Phylogenet. Evol. 61, 255–264.